NASA TECHNICAL NOTE

NASA TN D-5473


NASA TN D-5473



# A TRANSFORMER OF CLOSELY SPACED PULSED WAVEFORMS HAVING A NONZERO AVERAGE VALUE

*by Janis M. Niedra*

*Lewis Research Center*
*Cleveland, Ohio*

NATIONAL AERONAUTICS AND SPACE ADMINISTRATION • WASHINGTON, D. C. • OCTOBER 1969

| | | |
|---|---|---|
| 1. Report No.<br>NASA TN D-5473 | 2. Government Accession No. | 3. Recipient's Catalog No. |
| 4. Title and Subtitle<br>A TRANSFORMER OF CLOSELY SPACED PULSED WAVEFORMS HAVING A NONZERO AVERAGE VALUE | | 5. Report Date<br>October 1969<br>6. Performing Organization Code |
| 7. Author(s)<br>Janis M. Niedra | | 8. Performing Organization Report No.<br>E-5185 |
| 9. Performing Organization Name and Address<br>Lewis Research Center<br>National Aeronautics and Space Administration<br>Cleveland, Ohio 44135 | | 10. Work Unit No.<br>120-27<br>11. Contract or Grant No.<br>13. Type of Report and Period Covered<br>Technical Note |
| 12. Sponsoring Agency Name and Address<br>National Aeronautics and Space Adminstration<br>Washington, D.C. 20546 | | 14. Sponsoring Agency Code |

15. Supplementary Notes

16. Abstract

With the use of diodes, transistors, and magnetic cores, a passive circuit was constructed that transformed the voltage, either up or down, of repeated positive or negative pulses. This circuit combined a pulse transformer with switching devices to effect a resonant flux reset. It could transform various pulsed waveforms that had a nonzero average value and were relatively closely spaced in time. The circuit provided direct-current isolation between multiple loads and between a load and the source, similar to a conventional transformer. Several experimental circuits were tested.

| | | | |
|---|---|---|---|
| 17. Key Words *(Suggested by Author(s))*<br>Pulse transforming circuit<br>Voltage average transformation<br>Resonant flux reset<br>Closely spaced pulses | 18. Distribution Statement<br>Unclassified - unlimited | | |
| 19. Security Classif. (of this report)<br>Unclassified | 20. Security Classif. (of this page)<br>Unclassified | 21. No. of Pages<br>27 | 22. Price*<br>$3.00 |

*For sale by the Clearinghouse for Federal Scientific and Technical Information Springfield, Virginia 22151

# A TRANSFORMER OF CLOSELY SPACED PULSED WAVEFORMS HAVING A NONZERO AVERAGE VALUE

by Janis M. Niedra

Lewis Research Center

## SUMMARY

With the use of diodes, transistors, and magnetic cores, a passive circuit was constructed that transformed the voltage, either up or down, of repeated positive or negative pulses. This circuit combined a pulse transformer with switching devices to effect a resonant flux reset. It could transform various pulsed waveforms that had a nonzero average value and were relatively closely spaced in time. The circuit provided direct-current isolation between multiple loads and between a load and the source, similar to a conventional transformer. Several experimental circuits were tested.

## INTRODUCTION

On occasion a need arises to drive a load, or multiple loads such as transistor switches in an inverter circuit configuration, from a source of repetitive positive or negative voltage pulses with the requirement of direct-current isolation from load to source and load to load. This isolation is usually provided by an ordinary pulse transformer. In such a transformer, the pulse spacing is limited by the ability of the flux in the core to return to its initial value before the arrival of the next pulse. Especially with low impedance sources and loads, the needed flux reset time is normally significantly greater than the pulse width. In the case of relatively closely spaced repetitive positive or negative pulses, an ordinary transformer will be driven toward magnetic saturation and, therefore, cannot be used.

A new voltage-transforming circuit was constructed to handle repetitive positive or negative pulses that may be relatively closely spaced in time and have a nonzero average value. The only power source of the circuit is the pulse source; its output has no direct-current voltage offset, and it provides the isolation of a transformer. The principles of operation and limitations of this circuit are given in the following sections,

along with a discussion of several experimental versions that were tested.

## BASIC OPERATION OF REPETITIVE PULSE TRANSFORMER

The transformer circuit to be described is in its simplest form a passive four-terminal network The circuit is passive in the sense that all of its output energy comes from the input voltage source. Its input voltage $v_i$ and output voltage $v_o$ are functions of time ideally related by $v_o = nv_i$, where the constant n is the turns ratio of the transformer. (All symbols are defined in appendix A.) Further, the circuit transforms the average value of the input. That is, if the average value of the input is $\bar{v}_i$, then the average value of the output is $\bar{v}_o = n\bar{v}_i$. As in a normal transformer, departures from the ideal case exist because of the effects of leakage inductances, winding capacitances, and resistive and core losses. In addition, there is a restriction on the permissible time variation of $v_i$ for this circuit.

The operation of the repetitive pulse transformer can be understood by considering the simplified circuit shown in figure 1. This is a partial circuit that will react to posi-

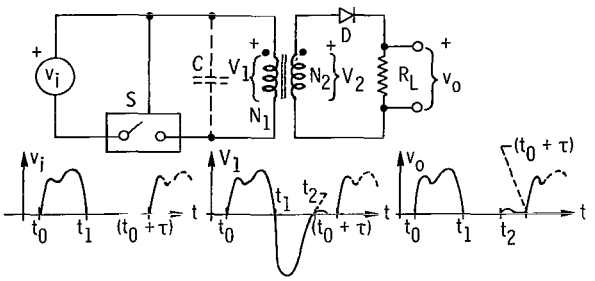


Figure 1. - Waveforms in a transformer of positive pulses.

tive pulses only; however, two such circuits can be combined, as shown later in the section Low-Frequency Bipolar Transformer, to form a bipolar transformer. The components are a switch S operated by the input $v_i$, a small capacitance C that may be the winding capacitance, a suitable transformer having $N_1$ primary and $N_2$ secondary turns, a diode D, and a load resistor $R_L$. By sensing $v_i$, the switch S remains closed if $v_i > 0$ and opens whenever $v_i \to 0$. When S is open, the $v_i$ is isolated from the circuit, and the primary winding is open circuited at S.

At time $t_0$, the magnetic core is resting at the point marked by $t_0$ on its characteristic of flux $\varphi$ against the magnetizing field H shown in figure 2. As $v_i$ rises, the switch S closes, and the flux increases along the path marked by the arrows. Since the diode D is forward biased, a transformed voltage $v_o = (N_2/N_1)v_i$ appears across the

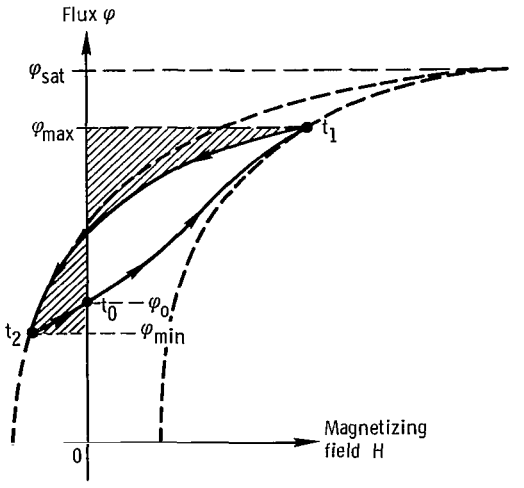


Figure 2. - Flux as function of H characteristic for core and cycled minor loop.

load $R_L$. The $\varphi$ reaches a maximum value $\varphi_{max}$ at time $t_1$, when $v_i$ falls to zero and S opens. At this time, the terminal voltage $v_1$ reverses polarity, which reverse biases D. Now the core sees a high impedance through the open switch, and $v_1$ performs a half cycle of an LC-type oscillation, which quickly resets the flux to the point marked $t_2$. The capacitance is provided by the distributed winding capacitance together with any external capacitance added across the primary winding, and the inductance is provided by the nonlinear path of $\varphi$ against H from point $t_1$ to point $t_2$. After time $t_2$, the diode D becomes forward biased, but $v_1$ ramains quite low because of the damping provided by $R_L$. The $v_o$ pulse appearing just after $t_2$ can be minimized by procedures discussed in connection with practical circuits. The flux has now returned to the starting point $t_0$. General voltage waveforms associated with this process are shown in figure 1 for repetitive pulses $v_i$ having a period of repetition $\tau$.

## LIMITATIONS OF REPETITIVE PULSE TRANSFORMER

This circuit is subject to more limitations and undesirable losses than a simple transformer. Use of semiconductor diodes in series with the load current introduces an obvious power loss. The switch S, which shall normally be a transistor, introduces an even greater series voltage drop and requires energy to operate. In certain cases, these semiconductors may set the limit to the maximum speed of response. There are, however, two additional restrictions as a consequence to the mode of operation of this circuit.

Magnetic saturation sets an upper limit to the voltage-time area $\int_{t_0}^{t_1} v_i \, dt$ that can be handled. But the present circuit used only a fraction of the available flux swing of the core material. Therefore, the mass of the core is increased by a factor that is the reciprocal of this fraction, assuming the same maximum voltage-time area capability. Thus, one should pick a core material having a substantial difference between the saturation and the remanent flux. For square loop cores, the introduction of a small air gap can reduce the remanent flux and make their use practical in this application.

When operating at the limit of maximum voltage-time area, the pulse repetition period $\tau$ must be great enough to let the core complete its flux reset; that is, $\tau \geq (t_2 - t_0)$ in figure 1. If the voltage-time area is less than the maximum permissible, then one may decrease $\tau$ below this limit, forcing the cycled minor loop in figure 2 to lie higher up on the core characteristic of $\varphi$ against H. The reset time $t_2 - t_1$ is the sum of the turnoff time $\tau_{off}$ of S (see fig. 3) and the duration of the oscillation. One can reduce the reset time by decreasing C, which compresses the reset oscillation. Such reduction of $t_2 - t_1$ is necessary to attain the highest permissible pulse repetition rate. It can also lead to the generation of very high voltages during reset, which can damage a switching transistor. These problems are discussed further in connection with optimum dissipation of the available energy of magnetization. This energy, which is proportional to the upper shaded area in figure 2, is returned to and partially or totally dissipated in the circuit external to the core.

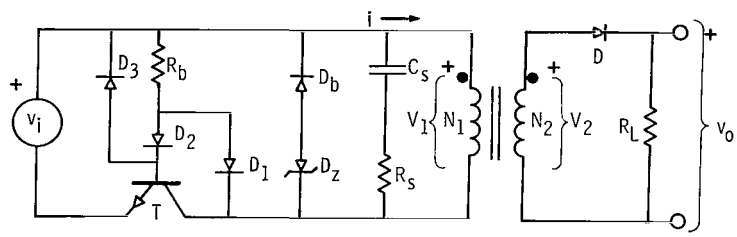


(a) Circuit.

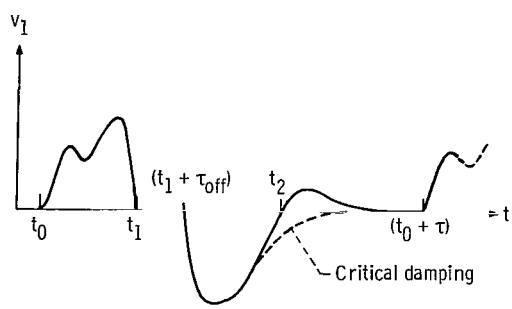


(b) Representative waveforms.

Figure 3. - Series version of practical pulse circuit.

# DESIGN CONSIDERATIONS

In general, the circuit design is dependent primarily on the core material and transistors that are employed. The nonlinear characteristics involved make it difficult to supply explicit values for circuit parameters. There is a broad range of voltage, power, pulse repetition rate, rise time, and other requirements from which specifications for a particular transformer could be selected. Thus, the circuit drawn in figure 1 may not work well in many cases without some modification. A high-repetition-rate circuit that can transmit undistorted pulses requires a well-designed pulse transformer and nondestructive dissipation of the available energy of magnetization in a time interval that may be less than the pulse duration. The latter problem is discussed in connection with the circuits of figures 3 and 4, which are somewhat more specific than the circuit in figure 1.

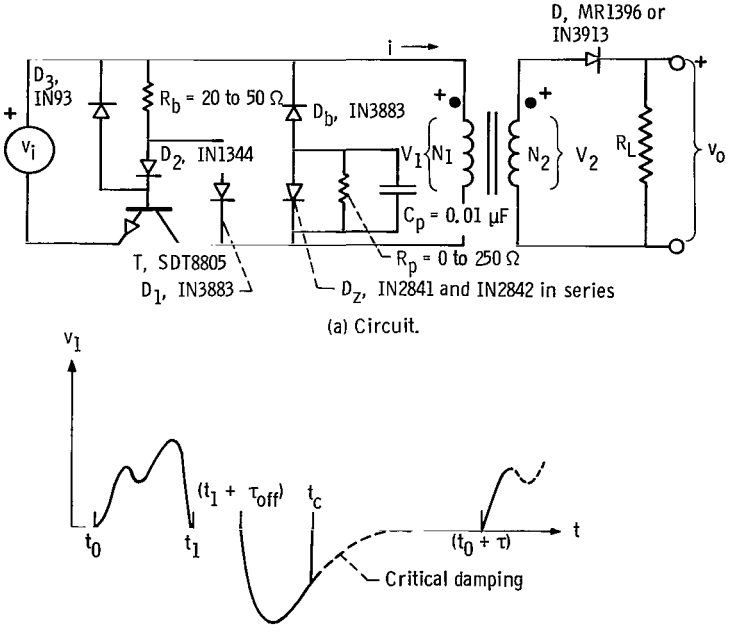


Figure 4. - Parallel version of practical pulse circuit.

## Circuit Energy Dissipation

Two practical types of circuits are now discussed. They differ in that one circuit uses a series resistor-capacitor connection, whereas the other connects these elements in parallel.

Series circuit. - Four new components, $D_b$, $D_z$, $R_s$, and $C_s$ were added to figure 3 to limit the peak voltage during flux reset and provide control over the dissipation of the available energy of magnetization. The zener diode $D_z$ keeps the voltage within the safe operating area of the transistor for a given maximum exciting current that the transistor must interrupt. The zener diode is isolated from the input $v_i$ by the diode $D_b$.

If the effects of the voltage drop in the winding resistance $R_w$ are neglected, as soon as $t$ exceeds $t_1$, $v_i = 0$, and $d\varphi/dt$ becomes negative. Because of stored charge, the transistor cannot turn off until the lapse of some turnoff time $\tau_{off}$. Therefore, the magnitude of $d\varphi/dt$ during this interval will be quite low if $R_w$ is small, there being a rapid rise after time $t_{off} = t_1 + \tau_{off}$. The available energy of magnetization thereafter starts to be partially dissipated in $R_w$ and $R_s$ and temporarily stored in $C_s$ and in an equivalent winding capacitance $C_w$. The terminal voltage $v_1$ reaches a negative peak and decays as $C_s$ discharges. Thus, at some time between $t_1$ and $t_2$, the exciting current $i_e$ reverses polarity and becomes negative. Unless $C_w$ is negligible, the current through $R_s$ will differ somewhat from $i_e$. This process dissipates a significant part of the available energy of magnetization in $R_s + R_w$.

Reversal of the polarity of $i_e$ implies that some of the energy stored in $C_s$ and $C_w$ is returned to the core. Appendix B shows that at time $t_2$

$$\int_{\varphi_{max}}^{\varphi_{min}} H \, d\varphi \leq 0 \tag{1}$$

the equality holding if $R_s = R_w = 0$. If the path $H = H(\varphi)$ is known and the equality holds, this equation determines $\varphi_{min}$. With reference to figure 2, equation (1) states that the shaded areas are equal if no losses exist in the winding and the external circuit. In this case, all the available energy of magnetization is put back into the core, which gives the minimum possible $\varphi_{min}$.

The flux rise from $\varphi_{min}$ to $\varphi_o$ may be quite small for cores having a significant remanent flux. Therefore, the additional flux reset generated by letting $i_e$ become negative can provide an increased available flux swing with these types of cores.

Solving for the voltages and currents for a general core is not feasible because the relation between $i_e$ and $\varphi$ is not necessarily linear. Whenever a linear relation such as

$$N_1 \frac{d\varphi}{di_e} = L \tag{2}$$

is valid, the flux reset is oscillatory in nature if

$$\frac{C_s R_s^2}{L} \leq 4 \tag{3}$$

At equality, there is critical damping. The inequality (3) is based on a simple RLC-type circuit which neglects $R_w$ and $C_w$. Sketches of representative terminal voltage waveforms are shown in figure 3(b) for the critically damped and oscillatory conditions. In the oscillatory case, one observes a positive voltage pulse across the load after time $t_2$. The magnitude of this pulse depends on the magnetic properties of the core and the circuit parameters, and its cause appears to be the flux rise from $\varphi_{min}$ to $\varphi_o$. Generally, $R_s$ and $C_s$ can be adjusted to minimize the reset time $t_2 - t_{off}$ subject to the peak voltage limitations of the transistor for a given size input pulse. If $D_z$ is a power zener diode, it too can be used to dissipate energy during flux reset.

Parallel circuit. - The circuit shown in figure 4(a) differs from the series circuit in that it uses a capacitor $C_p$ and a resistor $R_p$ in parallel to control the flux reset. The diode $D_b$ isolates now not only $D_z$ but also the $C_p$-$R_p$ combination from the input $v_i$. A major difference between the parallel circuit and the series circuit is that, in the parallel circuit, neglecting the effects of $C_w$, the exciting current $i_e$ cannot become negative.

The action of the diode $D_b$ is now considered in greater detail. If the flux reset is oscillatory, there exists a time $t_c$, where $t_{off} < t_c < t_2$, at which $i_e$ passes through zero. If $C_w$ is neglected, $i_e$ is then also the current at the terminals of $N_1$. Because $D_b$ prevents the flow of a negative $i_e$, the oscillation of $v_1$ ends discontinuously at time $t_c$. At this time, the flux has returned to $\varphi_o$, and $i_e = 0$. Thus, for the parallel circuit, $\varphi_{min} = \varphi_o$ and point $t_2$ coincides with point $t_0$ in figure 2 if $C_w = 0$. For any real circuit, $C_w \neq 0$, so that $d\varphi/dt$ does not go discontinuously to zero at time $t_c$, although the drop can be quite abrupt. The winding capacitance $C_w$ appears to be the cause of a small positive terminal voltage pulse that is observable under some conditions just after $t_c$.

The charge left on $C_p$ at time $t_c$ thereafter decays through $R_p$ with a time constant $R_pC_p$. As $R_p$ is increased, the $t_c$ decreases until it approaches the time at which $v_1$ peaks. An increase in $R_p$ decreases the reset time $t_c - t_{off}$ at the expense of generating a higher peak $v_1$. Since the $R_p$-$C_p$ combination is isolated from $v_i$ by $D_b$, the start of the next pulse may be immediately after $t_c$ if the pulse width is at least several times $R_pC_p$.

If equation (2) holds, the condition analogous to the inequality (3) for the parallel circuit is

$$\frac{L}{C_pR_p^2} \leq 4 \tag{4}$$

Representative waveforms are shown in figure 4(b).

Little of the available energy of magnetization can be returned to the core in this circuit, and, consequently, the parallel circuit minimizes the undesirable positive voltage pulse, such as is shown after time $t_2$ in figure 3(b) for the series circuit. Thus, the parallel circuit may have the advantage of a better reproduction of the input waveform. The parallel circuit is also suited for use with cores having an inherently low remanent flux. In such cores, the final flux level $\varphi_0$ will be low, also, and no extra flux swing capability can be produced by the application of a negative H. However, with higher remanence cores, the series circuit would have a bigger available flux swing. In some applications, the isolation of $C_p$ and $R_p$ from the input $v_i$ may favor the parallel circuit.

Energy transmission efficiency. - The total losses in these circuits consist of core loss, copper loss in the windings, losses in the semiconductors, and dissipation of the available energy of magnetization. Calculating the efficiency $\epsilon$ in general is difficult because of uncertainties associated with the semiconductors and the nonlinear properties of the core. It seems true, however, that the nonrecovery of the available energy of magnetization can account for a significant part of the total losses in certain cases.

Assuming a linear lossless core, one can calculate an upper bound for $\epsilon$. The energy of magnetization $E_{mag}$ for such a core is $\frac{1}{2}LI^2$, which is also the available energy of magnetization, as previously defined, because the core is lossless. Thus, in terms of the secondary voltage $v_2$,

$$E_{mag} = \frac{1}{2}\left(\frac{\bar{l}}{\mu AN_2^2}\right)\left(\int_{t_0}^{t_1} v_2\, dt\right)^2 \tag{5}$$

where $\mu$ is the total permeability, A is the cross section, and $\bar{l}$ is the mean length of the magnetic path of the core. The efficiency $\epsilon$ of the circuit must satisfy

$$\epsilon < \frac{E_L}{E_L + E_{mag}} \tag{6}$$

where

$$E_L = \frac{1}{R_L} \int_{t_0}^{t_1} v_o^2 \, dt \tag{7}$$

because other losses are omitted from the inequality (6). For a rectangular voltage pulse and $v_o \approx v_2$, the inequality (6) becomes

$$\epsilon < \frac{1}{1 + \frac{1}{2}\left(\frac{\bar{l}}{\mu A N_2^2}\right) R_L (t_1 - t_0)} \tag{8}$$

## Power Switching Requirements

The only switching elements investigated for use in the present circuits were transistors; gate-controlled rectifiers were unsuitable because they could not easily interrupt a flowing current. This necessity to stop the peak magnetizing current under conditions in which the $v_1$ may reach over 100 volts in a few microseconds places severe demands on the transistor in a circuit using a high exciting current core. As used herein, the transistor may need a significantly higher $V_{CEO}$ rating than the actual peak reset $v_1$ because the circuit encourages the phenomenon of reverse-bias second breakdown (ref. 1) The problem is more severe if a fast turnoff time $\tau_{off}$ is desired, because the higher speed power switching transistors are more susceptible to the second breakdown. Ideally, for a fast-rise-time power circuit, one would pick a switching transistor having a high $V_{CEO}$ rating, sufficient power and current capabilities, and the minimum-gain bandwidth product $f_t$ consistent with the desired speed. Limitation of the rate of rise and peak $v_1$ by use of the external capacitors has kept the voltages and currents within the safe operating area of the transistor in several experimental circuits.

Diodes $D_1$ and $D_2$ shown in figures 3 and 4 are used as feedback clamps to keep the collector out of saturation (ref. 2). Their presence increases the collector-to-emitter voltage drop but considerably reduces $\tau_{off}$. A germanium diode $D_3$ reduces reverse leakage and speeds sweepout of stored charge. A $\tau_{off}$ as low as 3 microseconds could be achieved for some power switching transistors such as the 2N3599 or the SDT8805.

## Significant Magnetic Properties of Core

The mode of operation of this pulse circuit requires a core having a substantial difference between its saturation and remanent flux. Low remanence results in a more complete utilization of the magnetic material and, hence, less core mass. Magnetically softer cores are preferred because the lower exciting current drawn by a more permeable core is easier to switch off.

Commercial supermalloy-tape-wound cores, which have the low direct current coercivity of about 0.8 ampere per meter (0.01 Oe), yielded a maximum available flux density swing of about 0.5 tesla compared with the saturation value of about 0.8 tesla. Magnetically soft square-loop materials such as supermendur can provide saturation flux densities of over 2 teslas, but because of their squareness, they are not useful in this circuit. The core can be modified by the introduction of an air gap to use a square-loop material. Appendix C shows that the introduction of an air gap equal to

$$l_{gap} = \frac{\mu_o H_c}{\alpha B_s} \bar{l} \tag{9}$$

in an ideally square-loop core will reduce it remanence from $B_s$ to $\alpha B_s$, where $0 < \alpha < 1$. The new saturation magnetomotive force $M_s$ is then

$$M_s = H_c \bar{l}(1 + \alpha^{-1}) \tag{10}$$

but the coercivity remains unchanged at $H_c$. If one assumes that all the available energy of magnetization can be returned to the core on reset, the minimum B reached will be

$$B_{min} = -B_s(1 - 2\alpha) \tag{11}$$

This value will also be the $B_o$ provided that $B_{min} \geq -\alpha B_s$, since the minimum possible $B_o$ is $-\alpha B_s$ in any case. From the equation

$$-\alpha B_s = -B_s(1 - 2\alpha) \tag{12}$$

one finds that there is no point in having an $\alpha$ less than 1/3 for the case of a lossless return of the energy of magnetization with this type of core. The maximum flux density swing is

$$(\Delta B)_{max} = B_s - B_{min} = 2B_s(1 - \alpha) \tag{13}$$

and it can be no bigger than

$$(\Delta B)_{max}\Big|_{\alpha=1/3} = \frac{4}{3} B_s \tag{14}$$

Use of the parallel $R_p$-$C_p$ combination precluded restoration of any energy to the core, so that circuits of that type can take advantage of an $\alpha < 1/3$. Even for the series $R_s$-$C_s$ circuit, the presence of losses and various hysteresis loop geometries can lead to a best $\alpha < 1/3$.

## EXPERIMENTAL CIRCUITS

Several circuits incorporating some of the ideas just discussed have been constructed. The very first bipolar transformer (ref. 3) had a rather large number of turns of fine wire that limited its frequency response and power handling capability. Now, two additional experimental circuits have been built, each of which can handle hundreds of watts of power. They were constructed from power components on hand without regard to optimization for any specific application.

### Low-Frequency Bipolar Transformer

The circuit detailed in figure 5 combines two single-polarity circuits in a way that enables it to handle both positive and negative repeated pulses. It was constructed around two rather large 2-mil supermalloy-tape-wound cores, each having an effective cross section of 10.37 square centimeters and a mean circumference of 35.7 centimeters. Each core was wound with four 100-turn windings of 12-gage wire and one 50-turn winding of 10-gage wire, from which various winding combinations could be selected. The outputs of $N_2$ can be combined across a split load or across a single load by uses of transistor switches as shown. Darlington connected transistors were used to increase the gain at the expense of a higher voltage drop. The use of the germanium diodes $D_2$

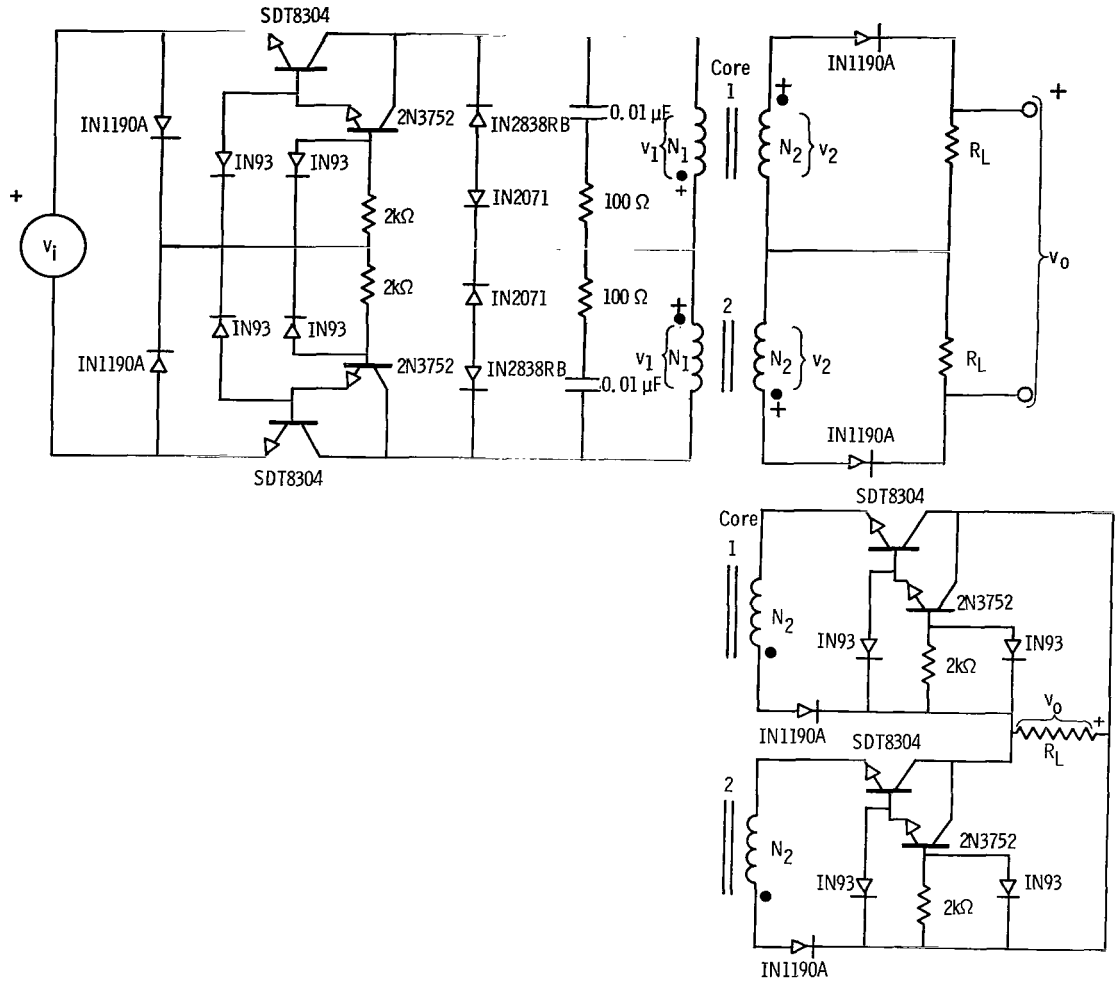


Figure 5. - Low-frequency bipolar pulse circuit. Cores 1 and 2, 50417-2F; each core includes four windings with 100 turns of 12-gage wire and one winding with 50 turns of 10-gage wire.

significantly reduced the reverse leakage and turnoff time of the transistors. The 40-ampere silicon rectifiers $D_1$ are relatively low reverse-leakage types suitable for low frequencies only.

Figure 6(a) shows the response of this circuit when excited by 20-volt rectangular positive pulses with a duration of 3 milliseconds and a period of repetition of 4 milliseconds. In this case, the load $R_L$ was 5 ohms, and $N_1 = N_2 = 100$ turns. The middle trace shows that about 17 volts was available at the output, the 3 volts being lost in winding resistances and semiconductor drops. Thus, 58-watt pulses were being delivered at a 75-percent duty factor. Testing at higher powers could not be done because the necessary power pulse generator was not available.

Distortion caused by semiconductor attenuation of low voltages is apparent with the triangular wave input shown in figure 6(b).

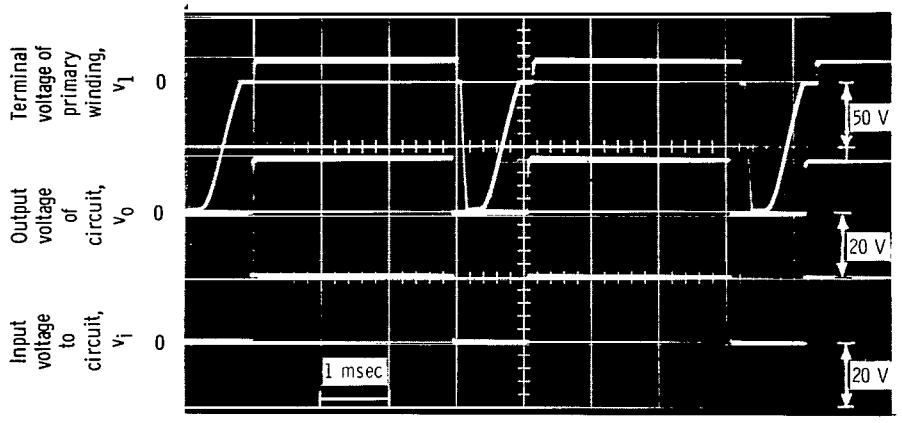


(a) Response to repeated positive pulses.

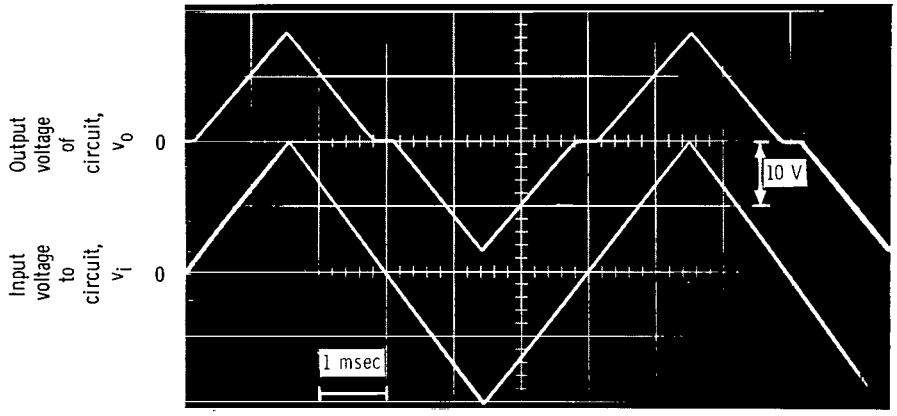


(b) Response to triangular wave.

Figure 6. - Response of the low-frequency bipolar transformer driving 5-ohm load.

## High-Frequency Unipolar Transformer

A simple circuit capable of responding to pulses narrower than 10 microseconds was constructed according to the diagram in figure 4. Four 24-turn windings of 14-gage wire were wound quadrifilar on a low-remanence powder core with a cross section of 7.26 square centimeters, a mean circumference of 24.8 centimeters, and a relative permeability of 150. This construction (see fig. 7) provided the low-capacitance tightly coupled windings needed for fast response.

It was necessary to use fast-recovery silicon power rectifiers such as the MR1396 or IN3913, which can handle 30 amperes and have a reverse recovery time of less than 0.2 microsecond. The use of the fast-recovery type IN3883 diode for $D_b$ and $D_1$ was also desirable. The presence of the antisaturation and carrier sweep-out diodes $D_1$, $D_2$, and $D_3$ reduced the $\tau_{off}$ of the SDT8805, which is a 30-ampere 300-volt transistor,

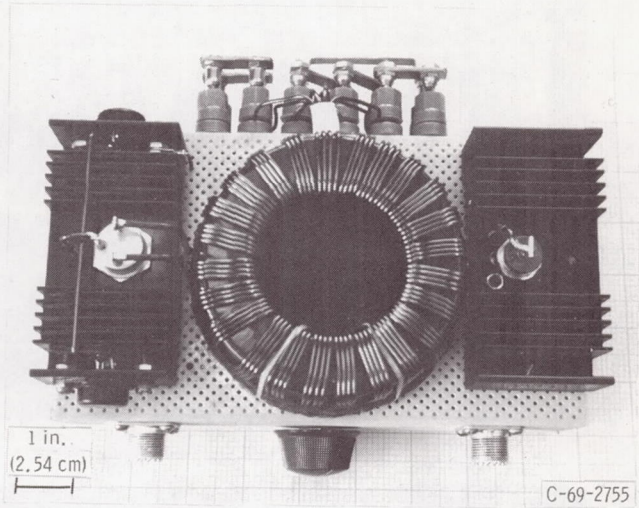


Figure 7. - Construction of high-frequency pulse transformer.

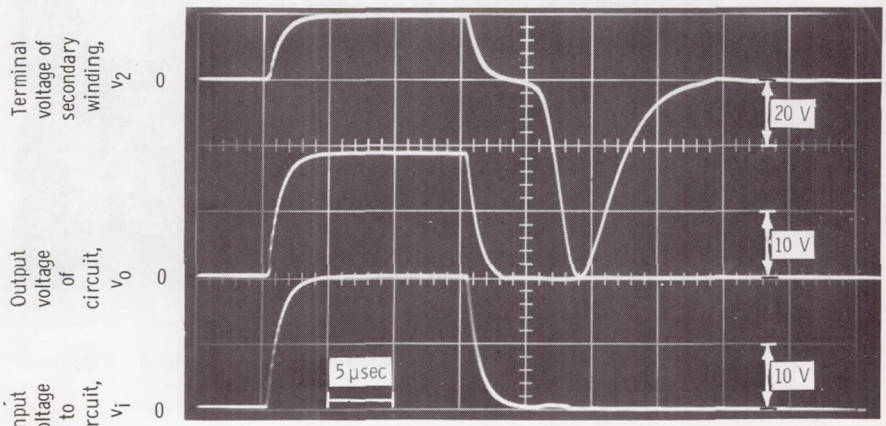


(a) Flux reset critically damped.

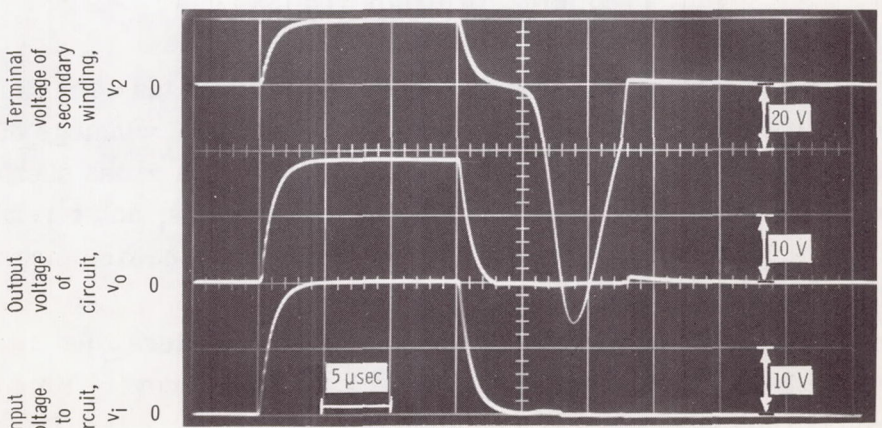


(b) Flux reset oscillatory.

Figure 8. - Typical response of high-frequency transformer with unity turns ratio and differing degrees of damping.

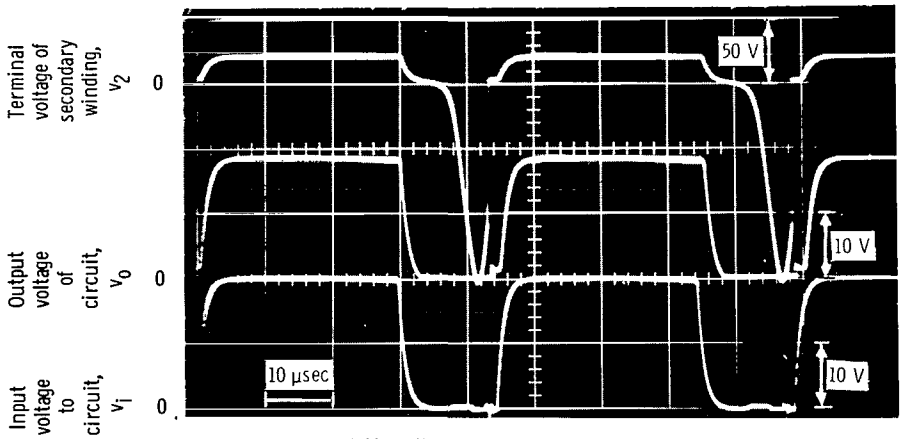


(a) 33-Watt pulses into 10-ohm load ($N_1 = N_2 = 24$).

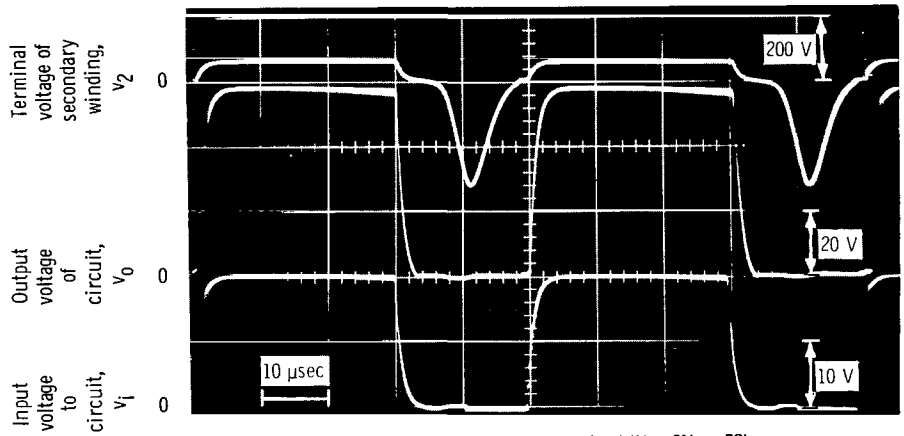


(b) 33-Watt pulses into 100-ohm load ($N_2 = 3N_1 = 72$).

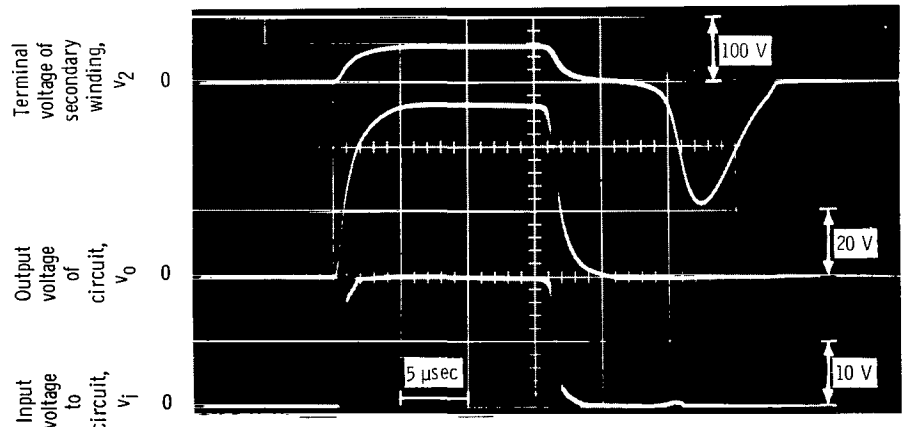


(c) 140-Watt pulse into 20-ohm load ($N_2 = 3N_1 = 72$).

Figure 9. - Response of high-frequency transformer at various power levels and loads.

to 3 or 4 microseconds. A 2N3599 was slightly faster at turnoff, but it has a maximum rating of only 100 volts.

Figure 8 illustrates some of the performance features observed when a 100-ohm load is driven with an applied $v_i$ of 20 volts amplitude and 15 microseconds duration. The turns ratio is 1:1, with $N_1 = 24$. Figures 8(a) and (b) compare the observed traces when $R_p$ was set for critical and less than critical damping, respectively. Thus, the turnoff and flux reset period could be compressed to slightly less than 10 microseconds.

The turns ratio, load, and pulse amplitude and duration were varied, and a few of the observations are presented in figure 9. The traces in figure 9(a) were observed while 33-watt pulses were delivered to a 10-ohm load at a duty factor greater than 50 percent and $N_1 = N_2$. The traces in figure 9(b) show pulses with the same duty factor delivering the same power to a 100-ohm load, with the transformer connected for a 3-to-1 stepup. The traces in figure 9(c) show a single 15-microsecond 140-watt pulse applied to a 20-ohm load. Testing at higher power levels and faster rise times could not be carried out for the lack of a suitable pulse generator.

Applying the inequality (8) gives $\epsilon < 0.68$ and $\epsilon < 0.95$ for the cases in figures 9(a) and (c), respectively.

## SUMMARY OF RESULTS

A circuit was constructed to transform the voltage, either up or down, of repeated positive or negative pulses. Transistors, diodes, resistors, capacitors, and magnetic cores were combined in a passive circuit that overcame the problem of magnetic saturation by providing a rapid resonant flux reset.

Similar to an ordinary transformer, this circuit could drive multiple direct-current isolated loads from a single source. It could transform various pulsed waveforms that have a nonzero average value and are relatively closely spaced in time. Thus, this circuit also transformed the average value of the input voltage. Its primary disadvantages are increased core mass due to incomplete use of the total available flux swing and an efficiency below that of an ordinary transformer. The lower efficiency resulted from semiconductor losses and the loss of the available energy of magnetization. In addition, there is a minimum permissible spacing in time between successive pulses. Because of voltage drops in the semiconductors, the circuits tested would not operate with inputs below about 1.5 volts.

The experimental circuits built demonstrated their feasibility to transmit hundreds of watts to resistive loads. Operation at a duty factor greater than 50 percent was observed at pulse widths of several milliseconds and 30 microseconds with two high-power

circuits. Finite turnoff time and the safe operating area of the power switching transistors were the chief limiting factors to the rate of pulse repetition.

One may be able to increase the efficiency and decrease the demands on the switching transistor by investigating variations on the circuits presented herein. For example, the possible advantages of a low-hysteresis, high-saturation, square-loop core with a small air gap may be significant in these circuits.

Lewis Research Center,
National Aeronautics and Space Administration,
Cleveland, Ohio, August 7, 1969,
120-27.

# APPENDIX A

## SYMBOLS

| | |
|---|---|
| $A$ | cross-sectional area of magnetic core |
| $B$ | magnetic flux density |
| $B_{max}$ | maximum B reached during cycle |
| $B_{min}$ | minimum B reached during cycle |
| $B_o$ | value of B at start of pulse |
| $B_s$ | saturation B for core |
| $(\Delta B)_{max}$ | maximum available change in B |
| $C$ | capacitance |
| $C_p, C_s$ | parallel and series capacitors, respectively, used to control flux reset |
| $C_w$ | winding capacitance |
| $D, D_b, D_1, D_2, D_3$ | diodes labeled in circuit diagrams |
| $D_z$ | zener diode |
| $E_L$ | energy delivered to load |
| $E_{mag}$ | energy of magnetization |
| $f_t$ | small-signal-gain bandwidth product of transistor |
| $H$ | magnetic field intensity |
| $H_c$ | coercivity of magnetic core |
| $i_e$ | exciting current of core |
| $L$ | inductance |
| $\bar{l}$ | mean length of magnetic path |
| $l_{gap}$ | length of gap cut in magnetic core |
| $M_s$ | saturation magnetomotive force of magnetic core |
| $N_1, N_2$ | number of turns on primary and secondary windings |
| $n$ | $N_2/N_1$ |
| $R_b$ | base resistor |

| | |
|---|---|
| $R_L$ | load resistor |
| $R_p, R_s$ | parallel and series resistors used to control flux reset |
| $R_w$ | winding resistance |
| S | switch |
| t | time variable |
| $t_0, t_1, t_2, t_{off}, t_c$ | critical times marked in cycle of operation |
| $V_{CEO}$ | collector-to-emitter breakdown voltage of transistor with base open circuited |
| $v_i$ | input voltage to circuit |
| $v_o$ | output voltage of circuit |
| $v_z$ | zener voltage of $D_z$ |
| $v_1, v_2$ | terminal voltages of primary and secondary windings |
| $\alpha$ | ratio of remanent-to-saturation magnetic flux density |
| $\epsilon$ | energy transmission efficiency of transformer |
| $\mu$ | total permeability of magnetic core |
| $\mu_o$ | permeability of free space |
| $\tau$ | period of pulse repetition |
| $\tau_{off}$ | turnoff time of transistor |
| $\varphi$ | magnetic flux |
| $\varphi_{max}$ | maximum $\varphi$ reached during cycle |
| $\varphi_{min}$ | minimum $\varphi$ reached during cycle |
| $\varphi_o$ | value of $\varphi$ at start of pulse |
| $\varphi_{sat}$ | saturation flux density |

Superscript:

average value

# APPENDIX B

## DERIVATION OF ENERGY BALANCE INEQUALITY

The derivation of inequality (1) is based on the equivalent circuit drawn in figure 10. This circuit is an approximation, valid during flux reset, to the actual series version of the pulse transformer circuit. The following three equations determine the voltages and currents as functions of time:

$$v_1 - R_w i_e - N_1 \frac{d\varphi}{dt} = 0 \tag{B1}$$

$$v_1 + R_s i_s + \frac{1}{C_s} \int_{t_{off}}^{t} i_s \, dx = 0 \tag{B2}$$

$$v_1 - \frac{1}{C_w} \int_{t_{off}}^{t} (i_s - i_e) dx = 0 \tag{B3}$$

where x (and later y) is a dummy variable of integration taking the place of the time variable t. These equations assume no initial charge on $C_s$ and $C_w$.

After substitution in equation (B1), the value for $v_1$, given by equation (B3) and multiplication by $i_e$, one obtains

$$N_1 i_e \frac{d\varphi}{dt} = -R_w i_e^2 + \frac{i_e}{C_w} \int_{t_{off}}^{t} (i_s - i_e) dx \tag{B4}$$

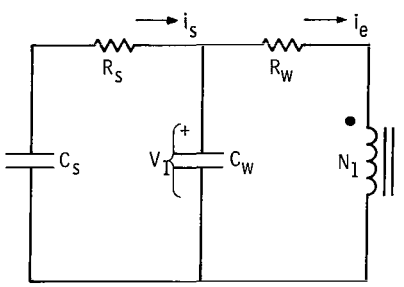


Figure 10. - Equivalent circuit for series version of pulse transformer during flux reset.

An integration from $t_{off}$ to $t$ transforms equation (B4) into

$$N_1 \int_{\varphi_{max}}^{\varphi} i_e \, d\varphi = -R_w \int_{t_{off}}^{t} i_e^2 \, dx + \frac{1}{C_w} \int_{t_{off}}^{t} i_e(y) \int_{t_{off}}^{y} \left[i_s(x) - i_e(x)\right] dx \, dy \qquad \text{(B5)}$$

It helps in later manipulations to add and subtract the terms $i_s(y)$ to $i_e(y)$ in equation (B5). This operation changes the form of equation (B5) to

$$N_1 \int_{\varphi_{max}}^{\varphi} i_e \, d\varphi = -R_w \int_{t_{off}}^{t} i_e^2 \, dx - \frac{1}{C_w} \int_{t_{off}}^{t} \left[i_s(y) - i_e(y)\right] \int_{t_{off}}^{y} \left[i_s(x) - i_e(x)\right] dx \, dy$$

$$+ \frac{1}{C_w} \int_{t_{off}}^{t} i_s(y) \int_{t_{off}}^{y} \left[i_s(x) - i_e(x)\right] dx \, dy \qquad \text{(B6)}$$

Before proceeding, a specialized formula for integration by parts is needed. Let $U(x)$ and $V(x)$ be arbitrary integrable functions of $x$. Then it is true that

$$\int_a^b V(y) \int_a^y U(x)dx \, dy = \left[\int_a^b U(x)dx\right]\left[\int_a^b V(x)dx\right] - \int_a^b U(y) \int_a^y V(x)dx \, dy \qquad \text{(B7)}$$

In the case $U(x) \equiv V(x)$, it follows immediately that

$$\int_a^b U(y) \int_a^y U(x)dx \, dy = \frac{1}{2}\left[\int_a^b U(x)dx\right]^2 \qquad \text{(B8)}$$

Returning now to (B6), one sees that, by letting $i_s - i_e = U$, applies to the first iterated integral on the right. Therefore,

$$N_1 \int_{\varphi_{max}}^{\varphi} i_e \, d\varphi = -R_w \int_{t_{off}}^{t} i_e^2 \, dx - \frac{1}{2C_w}\left[\int_{t_{off}}^{t} (i_s - i_e)dx\right]^2$$

$$+ \frac{1}{C_w} \int_{t_{off}}^{t} i_s(y) \int_{t_{off}}^{y} [i_s(x) - i_e(x)]dx \, dy \qquad \text{(B9)}$$

According to equation (B3), the second integral on the right side of equation (B9) is just $C_w v_1$. Further, from equations (B2) and (B3), it follows that

$$\frac{1}{C_w} \int_{t_{off}}^{y} (i_s - i_e)dx = -R_s i_s(y) - \frac{1}{C_s} \int_{t_{off}}^{y} i_s \, dx \qquad \text{(B10)}$$

which can be substituted in the iterated integral in equation (B9). After these substitutions, the result is

$$N_1 \int_{\varphi_{max}}^{\varphi} i_e \, d\varphi = -R_w \int_{t_{off}}^{t} i_e^2 \, dx - \frac{1}{2} C_w v_1^2 - R_s \int_{t_{off}}^{t} i_s^2 \, dy$$

$$- \frac{1}{C_s} \int_{t_{off}}^{t} i_s(y) \int_{t_{off}}^{y} i_s(x)dx \, dy \qquad \text{(B11)}$$

Formula (B8) again applies to the iterated integral. The general result proved thus is the energy balance equation

$$N_1 \int_{\varphi_{max}}^{\varphi} i_e \, d\varphi = -R_w \int_{t_{off}}^{t} i_e^2 \, dx - R_s \int_{t_{off}}^{t} i_s^2 \, dx - \frac{1}{2} C_w v_1^2 - \frac{1}{2C_s}\left[\int_{t_{off}}^{t} i_s \, dx\right]^2 \qquad \text{(B12)}$$

In particular, equation (B12) is valid at time $t_2$ when $\varphi = \varphi_{min}$ and $d\varphi/dt = 0$. If $R_w$ and $R_s$ are not both equal to zero, then (B12) requires that

$$\int_{\varphi_{max}}^{\varphi_{min}} i_e \, d\varphi < 0 \tag{B13}$$

If $R_w = R_s = 0$, then $v_1(t_2) = i_e(t_2)R_w = 0$ from (B1), $\int_{t_{off}}^{t_2} i_s \, dx = 0$ from (B2), and, consequently, (B12) reduces to

$$\int_{\varphi_{max}}^{\varphi_{min}} i_e \, d\varphi = 0 \tag{B14}$$

Inequality (B13) together with the equality (B14) constitute the desired result.

# APPENDIX C

## EFFECTS OF AIR GAP IN SQUARE-LOOP CORE

An ideally square-loop core has a saturation flux density $B_s$ and a coercivity $H_c$. An air gap of length $l_{gap}$ is cut into the core such that $l_{gap}$ is small compared with the mean length $\bar{l}$ of magnetic path of the core. Also assumed is that $l_{gap}$ is sufficiently small to provide a uniform field $B_g$ in the gap. The core is equipped with an N-turn winding carrying a current i.

With fields in the core material denoted by the subscript m and fields in the air gap by the subscript g, Ampere's circuital law states that

$$H_m\bar{l} + H_g l_g = Ni \tag{C1}$$

Continuity of flux requires that, under the assumption of a uniform gap field,

$$B_m = B_g = \mu_o H_g \tag{C2}$$

Eliminating $H_g$ between (C1) and (C2) results in

$$H_m\bar{l} + \frac{B_m}{\mu_o} l_g = Ni \tag{C3}$$

Note that, if the core is not saturated (i.e., $B_m = \alpha B_s$ where $0 < \alpha < 1$), then

$$H_m = \pm H_c$$

Consider now the case $i = 0$ and assume that the air gap is large enough to reduce the remanent flux density from $B_s$ to $\alpha B_s$. Then by equation (C3),

$$-H_c\bar{l} + \frac{\alpha B_s}{\mu_o} l_g = 0 \tag{C4}$$

and the length of the air gap is given by

$$l_g = \frac{\mu_o H_c}{\alpha B_s} \bar{l} \tag{C5}$$

Let the length of the air gap be given by (C5) and suppose that the current i is just large enough to saturate the core. Then, $H_m = H_c$ and $B_m = B_s$. Substitution of these values in equation (C3) yields the saturation magnetomotive force

$$M_s = H_c \bar{l} \left(1 + \frac{1}{\alpha}\right) \tag{C6}$$

## REFERENCES


1. Anon.: Power Transistor Handbook. Motorola, Inc., 1961, Sections 2-15 and 2-16.
2. Greiner, Richard A.: Semiconductor Devices and Applications. McGraw-Hill Book Co., Inc., 1961, pp. 382-383.
3. Niedra, Janis M.: A Passive Isolating Transformer of Repeated Positive or Negative Voltage Pulses. Proc. IEEE, vol. 56, no. 10, Oct. 1968, pp. 1754-1755.

*"The aeronautical and space activities of the United States shall be conducted so as to contribute . . . to the expansion of human knowledge of phenomena in the atmosphere and space. The Administration shall provide for the widest practicable and appropriate dissemination of information concerning its activities and the results thereof."*

—NATIONAL AERONAUTICS AND SPACE ACT OF 1958

# NASA SCIENTIFIC AND TECHNICAL PUBLICATIONS

TECHNICAL REPORTS: Scientific and technical information considered important, complete, and a lasting contribution to existing knowledge.

TECHNICAL NOTES: Information less broad in scope but nevertheless of importance as a contribution to existing knowledge.

TECHNICAL MEMORANDUMS: Information receiving limited distribution because of preliminary data, security classification, or other reasons.

CONTRACTOR REPORTS: Scientific and technical information generated under a NASA contract or grant and considered an important contribution to existing knowledge.

TECHNICAL TRANSLATIONS: Information published in a foreign language considered to merit NASA distribution in English.

SPECIAL PUBLICATIONS: Information derived from or of value to NASA activities. Publications include conference proceedings, monographs, data compilations, handbooks, sourcebooks, and special bibliographies.

TECHNOLOGY UTILIZATION PUBLICATIONS: Information on technology used by NASA that may be of particular interest in commercial and other non-aerospace applications. Publications include Tech Briefs, Technology Utilization Reports and Notes, and Technology Surveys.

*Details on the availability of these publications may be obtained from:*

**SCIENTIFIC AND TECHNICAL INFORMATION DIVISION**

**NATIONAL AERONAUTICS AND SPACE ADMINISTRATION**

**Washington, D.C. 20546**